Int. J. Solids Structures, 1974, Vol. 10, pp. 389–400. Pergamon Press. Printed in Gt. Britain.

THE DEPENDENCE OF SHEAR LAG ON PARTIAL INTERACTION IN COMPOSITE BEAMS

A. O. ADEKOLA†

Department of Civil Engineering, University of Lagos, Nigeria

(*Received* 15 *September* 1972; *revised* 8 *May* 1973)

Abstract—In this paper, the constitutive equations which relate partial interaction with shear lag are formulated and solved by series solutions for deflexion and in-plane stress in the slab to satisfy all the known boundary conditions. The results clearly demonstrate the influence of flexible shear connectors used in composite beams and also show that a more rational basis for defining effective width is from deflexion considerations. This shows that effective width increases with increasing degree of interaction, i.e. as the number of flexible shear connectors is increased. It is also established that there is a limiting degree of interaction beyond which deflexion is not sensibly influenced.

INTRODUCTION

The treatment of the problem of the dependence of shear lag on partial interaction in composite beams of steel and concrete is little understood from the classical elasticity point of view. Severely approximate solutions exist which either treat partial interaction alone, ignoring shear lag effects[5], or shear lag effects alone without a consideration of partial interaction[4].

Here a composite beam system of several equally spaced simply supported steel beams supporting and connected with a concrete slab, as shown in Fig. 1, is considered. Vertical midspan point loads applied at the slab-beam junctions and superimposed live load applied on the slab were considered.

Concrete is not truly an elastic material so that the analytical treatment of a member made of concrete is often difficult whether as an isotropic case or as an orthotropic case, both of which assume linear elasticity. In this paper, for convenience, the concrete slab has been treated within the classical theory for isotropic materials. The general case of orthotropic material does not require a new or more complex method of solution.

Finally mention must be made of an earlier paper[4] in which edge and interaction effects were ignored. These simplifying assumptions are dropped in the present paper.

GOVERNING EQUATIONS

Let $(x, y) = (x_1, x_2)$ be the two-dimensional coordinates. The bending and torsional moments due to the action of a discontinuous load distribution in an isotropic plate are given by:

$$\left.\begin{aligned} M_{11} &= -g(w_{,11} + \mu w_{,22}), \\ M_{22} &= -g(w_{,22} + \mu w_{,11}), \\ M_{12} &= -g(1-\mu)w_{,12}, \end{aligned}\right\} \tag{1}$$

† Professor and Head of Civil Engineering.

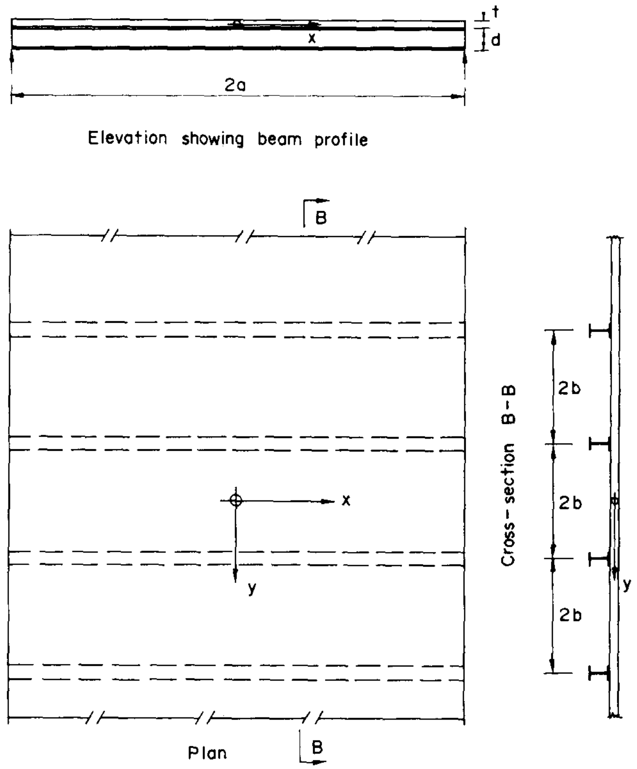

Fig. 1.

provided that the deflexion $w(x, y)$ satisfies the equation

$$g\nabla^4 w = q(x, y), \tag{2}$$

where ∇^4 denotes the two-dimensional biharmonic operator. In (1) and (2), $q(x, y)$ is the prescribed load, μ and g respectively stand for the Poisson's ratio and the flexural rigidity of the plate, while a comma followed by an index indicates partial differentiation with respect to the corresponding variable. Once the bending and torsional moments are known the membrane stresses are readily computable.

For a complete description of the stress distribution in the plate, we adjoin to (1) and (2) the stresses and displacements which are representable in terms of the Airy's stress function by means of

$$\left.\begin{aligned} \sigma_{11} &= \phi_{,22} \\ \sigma_{22} &= \phi_{,11} \\ \sigma_{12} &= -\phi_{,12} \\ 2G(1+\mu)U_{1,1} &= \sigma_{11} - \mu\sigma_{22} \\ 2G(1+\mu)U_{2,2} &= \sigma_{22} - \mu\sigma_{11} \end{aligned}\right\} \tag{3}$$

where (U_1, U_2) denotes the displacement vector, G the shear modulus, while the function ϕ satisfies the biharmonic equation

$$\nabla^4\phi = 0. \tag{4}$$

The preceding equations are to be accompanied by appropriate boundary conditions. In particular, if the domain $|x| < a$, $|y| < \infty$ is occupied by an isotropic plate which is simply supported along the edges, then we have

$$w = M_{11} = 0 \tag{5}$$

when $x = \pm a$, $y = \pm(2n-1)b$, $n = 1, 2, 3$.

The condition of stress-free edges also implies that

$$\sigma_{11} = \sigma_{12} = 0 \tag{6}$$

when $x = \pm a$, $|y| < \infty$, while symmetry consideration imposes the conditions

$$U_2 = w_{,2} = 0 \tag{7}$$

for $|x| < a$, $y = 0$.

The equilibrium equation has been shown [4] to be given by

$$-E_s I_s w_{,1111} - Q_{c,1} + \frac{d}{2} \cdot F_{,11} + p^1 = 0 \tag{8}$$

where

$$-E_s I_s w_{,11} = M_s \quad \text{and} \quad Q_{c,1} = -2g\nabla^2 w_{,2}.$$

The compatibility condition can be deduced from the assumption that the slip, ε, is related to the common interface differential strain, as well as the interacting slab in-plane force and the steel beam axial force in the following manner:

$$k_s^{-1}F_{,11} = \varepsilon_{,1} = e_s - e_c.$$

On substituting for e_s and e_c, this becomes

$$(E_s A_s)^{-1}F + \frac{d}{2} w_{,11} - E_c^{-1}(\phi_{,22} - \mu\phi_{,11}) + \frac{t}{2} w_{,11} = k_s^{-1}F_{,11} \tag{9}$$

in which

$$F = -2\phi_{,2}|_{y=b}.$$

Equations (8) and (9) are valid at the slab-beam junctions only.

ANALYSIS

Guided by the formulation of the problem, we assume that $q(x, y)$ admits the Fourier series representation

$$q(x, y) = g \sum_{n=1}^{\infty} q_n \cos \alpha_n x \tag{10}$$

where

$$\alpha_n = (2n-1)\pi/2a \quad \text{and} \quad q_n = 2\alpha_n^{-1}(-1)^{n+1}q/ga.$$

The substitution of (10) into (2) gives a general solution for w in the form

$$w = \sum_{n=1}^{\infty} \cos \alpha_n x[\alpha_n^{-4}q_n + A_n \cosh(\alpha_n y) + B_n y \sinh(\alpha_n y)], \tag{11}$$

where A_n and B_n are two arbitrary superposition coefficients. It is easily verified that the choice of (11) ensures the automatic satisfaction of the two conditions in (5), as well as the second condition in (7).

We now take the general solution of (4) in the form

$$\phi = \sum_{n=1}^{\infty} \cos(\alpha_n x)[A_n^* \cosh \alpha_n y + B_n^* y \sinh \alpha_n y] + \sum_{n=1}^{\infty} \cos(\lambda_n y)[a \sinh \lambda_n a \cosh \lambda_n x - x \sinh \lambda_n x \cosh \lambda_n a]C_n^* \quad (12)$$

where A_n^*, B_n^* and C_n^* are three as yet arbitrary superposition coefficients and

$$\lambda_n = (2n-1)\pi/b.$$

It is easily shown that the displacement component, deducible from (3) and (12) by straightforward integration and differentiation, satisfies the remaining condition in (7), while the normal stress σ_{11} also satisfies the first condition in (6).

The satisfaction of the symmetry conditions

$$U_2 = w_{,2} = 0$$

on ($y = \pm b$, $|x| < a$) now yields

$$\left.\begin{aligned} \alpha_n A_n &= -\{1 + \alpha_n b \coth(\alpha_n b)\}B_n \\ \alpha_n A_n^* &= \{(1-\mu)/(1+\mu) - \alpha_n b \coth(\alpha_n b)\}B_n^*, \end{aligned}\right\} \quad (13)$$

while the vanishing of the shear stress σ_{12} at the edges $x = \pm a$, $|y| < \infty$ yields the series equation

$$\sum_{n=1}^{\infty} D_n^* \sin \lambda_n y = \sum_{m=1}^{\infty} (-1)^{m+1}\alpha_m\{\alpha_m A_m^* \sinh \alpha_m y + B_m^*(\sinh \alpha_m y + \alpha_m y \cosh \alpha_m y)\} \quad (14)$$

on setting

$$D_n^* = C_n^*\{\sinh \lambda_n a \cosh \lambda_n a + \lambda_n a\}\lambda_n. \quad (15)$$

If we now multiply both sides of (14) by $\sin(\lambda_r y)$ and then integrate with respect to y from $-b$ to b (assuming that the integration and summation signs can be interchanged), we may make use of well-known trigonometric orthogonality relations and the definite integrals

$$\left.\begin{aligned} &\int_{-b}^{b} \sinh(\alpha_n y)\sin(\lambda_r y)\, dy = 2\lambda_r(\lambda_r^2 + \alpha_n^2)^{-1} \sinh(\alpha_n b), \\ &\int_{-b}^{b} y \cosh(\alpha_n y)\sin(\lambda_r y)\, dy = 2\lambda_r(\lambda_r^2 + \alpha_n^2)^{-2}[b(\lambda_r^2 + \alpha_n^2)\cosh(\alpha_n b) - 2\alpha_n \sinh(\alpha_n b)] \end{aligned}\right\} \quad (16)$$

to arrive at

$$C_n^*[\sinh(\lambda_n a)\cosh(\lambda_n a) + \lambda_n a]\lambda_n = 2\sum_{r=1}^{\infty} [(1+\mu)^{-1}\alpha_r^{-1} - \alpha_r(\alpha_r^2 + \lambda_n^2)^{-1}]F_{nr} B_r^* \quad (17)$$

where

$$F_{nr} = 2(-1)^{r+1}\lambda_n \alpha_r^2 b^{-1}(\alpha_r^2 + \lambda_n^2)^{-1} \sinh(\alpha_r b). \quad (18)$$

Assuming now that the function p^1 admits the Fourier series representation

$$p^1 = \sum_{n=1}^{\infty} p_n \cos(\alpha_n x), \quad (19)$$

application of the equilibrium equation (8) at $y = \pm b$, $|x| < a$ then yields

$$B_n J_n = E_s I_s q_n - p_n - 2td\alpha_n^2(1+\mu)^{-1}\sinh(\alpha_n b), B_n^* \tag{20}$$

where

$$J_n = \alpha_n^2\left\{\alpha_n E_s I_s\left(\cosh\alpha_n b + \frac{\alpha_n b}{\sinh\alpha_n b}\right) + 4g\sinh a_n b\right\}. \tag{21}$$

It remains to satisfy the compatibility condition (9) at the slab-beam junctions. On performing straightforward algebraic manipulations, we obtain

$$\begin{aligned}
&-4t(1+\mu)^{-1}\sum_{m=1}^{\infty}\cos\alpha_m x\sinh\alpha_m b\{(E_s A_s)^{-1} + k_s^{-1}\alpha_m^2\}B_m^* \\
&-\frac{(\mathrm{d}+t)}{2}\sum_{m=1}^{\infty}\alpha_m^2\cos\alpha_m x\left\{\alpha_m^{-4}q_m - \alpha_m^{-1}B_m\left(\cosh\alpha_m b + \frac{\alpha_m b}{\sinh\alpha_m b}\right)\right\} \\
&-E_c^{-1}\sum_{m=1}^{\infty}\alpha_m\cos\alpha_m x\left\{(3+\mu)(1+\mu)^{-1}\cosh\alpha_m b - \frac{\alpha_m b}{\sinh\alpha_m b}\right\}B_m^* \\
&-\mu E_c^{-1}\sum_{m=1}^{\infty}\alpha_m^2\cos\alpha_m x\left\{(1-\mu)(1+\mu)^{-1}\cosh\alpha_m b - \frac{\alpha_m b}{\sinh\alpha_m b}\right\}B_m^* \\
&= E_c^{-1}\sum_{n=1}^{\infty}\lambda_n^2\{a\sinh(\lambda_n a)\cosh(\lambda_n x) - x\sinh(\lambda_n x)\cosh\lambda_n a\}C_n^* \\
&+\mu E_c^{-1}\sum_{n=1}^{\infty}\lambda_n\{\cosh(\lambda_n x)(\lambda_n a\sinh\lambda_n a - 2\cosh\lambda_n a) - \lambda_n x\sinh\lambda_n x\cosh\lambda_n a\}C_n^*
\end{aligned} \tag{22}$$

on $y = b$ and for $|x| < a$.

The superposition coefficients B_n, and B_n^* in this equation can easily be taken out from under the summation signs. To this end, we multiply both sides of (22) by $\cos\alpha_r x$ and then integrate with respect to x from $-a$ to a. With the aid of well-known orthogonality relations and the easily checked results

$$\left.\begin{aligned}
&\int_{-a}^{a}\cosh(\lambda x)\cos(\alpha_n x)\,\mathrm{d}x = 2\alpha_n(-1)^{n+1}(\alpha_n^2+\lambda^2)^{-1}\cosh\lambda a, \\
&\int_{-a}^{a}x\sinh\lambda x\cos\alpha_n x\,\mathrm{d}x = 2\alpha_n(-1)^{n+1}(\alpha_n^2+\lambda^2)^{-2}\{a(\alpha_n^2+\lambda^2)\sinh\lambda a - 2\lambda\cosh\lambda a)\}
\end{aligned}\right\} \tag{23}$$

one arrives at the equation

$$B_m^* = B_m^{*(o)} + 4E_c^{-1}(-1)^{m+1}\alpha_m V_m\sum_{n=1}^{\infty}\lambda_n\cosh^2\lambda_n a\frac{\mu\alpha_m^2 - \lambda_m^2}{(\alpha_m^2+\lambda_n^2)^2}\cdot C_n^* \tag{24}$$

where

$$\begin{aligned}
V_m^{-1} &= \alpha_m^3 adt(d+t)(1+\mu)^{-1}(\alpha_m b + \sinh\alpha_m b\cosh\alpha_m b)J_m^{-1} \\
&+ 4at(1+\mu)^{-1}\sinh\alpha_m b\{(E_s A_s)^{-1} + \alpha_m^2 k_s^{-1}\} \\
&+ E_c^{-1}\alpha_m a\left\{(3-\mu)\cosh\alpha_m b - (1+\mu)\frac{\alpha_m b}{\sinh\alpha_m b}\right\}
\end{aligned} \tag{25}$$

while

$$B_m^{*(o)} = -\frac{a(d+t)}{2} V_m J_m^{-1}\left\{\alpha_m p_m\left(\cosh \alpha_m b + \frac{a_m b}{\sinh \alpha_m b}\right) + 4gq_m \sin \alpha_m b\right\}. \tag{26}$$

If we now introduce the additional auxiliary notations

$$\left.\begin{aligned} H_{nm} &= \frac{8(-1)^{m+1}\alpha_m V_m(\mu\alpha_m^2 - \lambda_n^2)(\alpha_m^2 + \lambda_n^2)^{-2} \cosh \lambda_n a}{E_c\{\sinh \lambda_n a \cosh \lambda_n a + \lambda_n a\}} \\ L_{nr} &= \{\alpha_r^{-1}(1+\mu)^{-1} - \alpha_r(\alpha_r^2 + \lambda_n^2)^{-1}\}F_{nr} \\ \Omega_{mr} &= \sum_{n=1}^{\infty} H_{mn} L_{nr}, \end{aligned}\right\} \tag{27}$$

the elimination of C_n^* between the two systems of equations given in equations (17) and (24) yields the following infinite system of equations for the unknowns B_m ($m = 1, 2, \ldots$):

$$B_m^* = B_m^{*(o)} + \sum_{r=1}^{\infty} \Omega_{mr} B_r^*. \tag{28}$$

Once the B_m^* have been determined, the superposition coefficients C_n^* and B_n follow from equations (17) and (20). Equations (28) are solved by the usual segmentation method according to which an $n \times n$ ($n = 5$ or 7) system of equations is considered.

It is apparent from equations (25) and (26) that the superposition coefficients B_n^*, and consequently all the other superposition coefficients of the stress and deflexion functions, depend on k_s which defines the degree of interaction.

Case of no interaction

In the absence of any interaction between the two elements, that is, when the loaded slab is merely resting on the beams and is not connected physically to them, the force of interaction F becomes zero; hence the superposition coefficients $A_n = B_n = C_n = 0$. An "indeterminate" strain incompatibility condition exists (see equation (9)). Under these conditions, the deflexion of the slab-beam system along the steel beams, i.e. at $y = \pm b$, then becomes:

$$w_o = \sum_{n=1}^{\infty} \cos \alpha_n x\left\{\alpha_n^{-1} p_n\left(\cosh \alpha_m b + \frac{a_m b}{\sinh \alpha_m b}\right) + 4\alpha_n q_n g \sinh \alpha_m b\right\} J_n^{-1}. \tag{29}$$

This is the deflexion equation at a rib of a system of elastically simply supported plate. The maximum central deflexion of this system is used as the reference for estimating deflexion factor γ_w for the partial interaction case.

The loading, span, sectional properties of the steel section, etc. used for computations are as follows:

Point load $p = 299$ kN.
Super load $q = (2{\cdot}873 + 0{\cdot}2265t)\,\text{kN/m}^2$, including slab self weight, where t is in cm.
Span $2a = 7{\cdot}63$ m.
Ribs are Universal Steel I—sections 610 × 228 mm × 137 N of
Area, A_s, $= 1{\cdot}789 \times 10^{-2}$ m^2, and second Moment of Area, I_s, $= 1{\cdot}12 \times 10^{-3}$ m^4.
Modulus of elasticity of steel $= 2{\cdot}085$ kN/cm^2.
Slab thickness $t = 152{\cdot}4$ mm.
Modular ratio between steel and concrete is taken as 10 and Poisson ratio as 0·2.

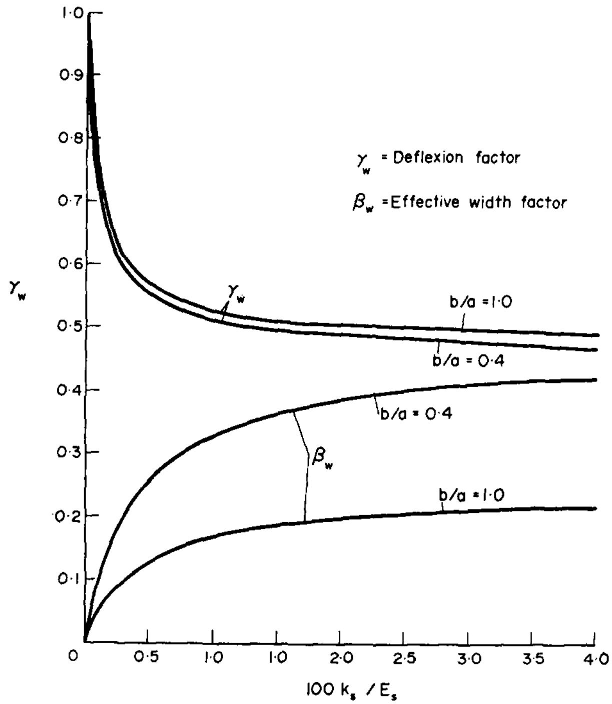

Fig. 2. Variation of γ_w and β_w with k_s for a point load at the centre.

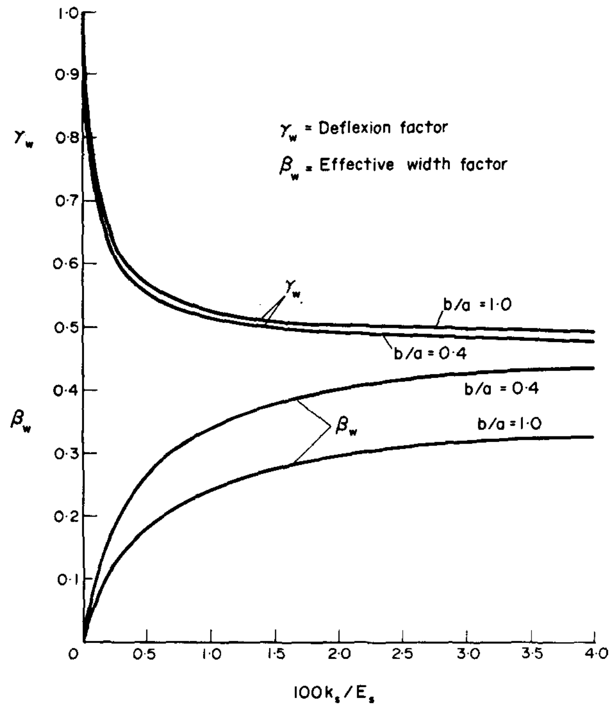

Fig. 3. Variation of γ_w and β_w with k_s for superimposed floor load.

Deflexion factor

Deflexion factor is defined as the ratio of the central deflexion at a rib when there is interaction and the central rib deflexion of the corresponding system of elastically rib-supported slab with identical rib and slab dimensions and material properties. This has been taken as a measure of the increased stiffness of the composite system and also as an exposition of the economics of composite construction (see Figs. 2 and 3).

$$\gamma_w = \frac{\sum_{n=1}^{\infty} \alpha_n^{-4}\{q_n - \alpha_n^3 B_n(\cosh \alpha_n b + \alpha_n b/\sinh \alpha_n b\}\cos \alpha_n x}{\sum_{n=1}^{\infty} \{\alpha_n^{-1} p_n(\cosh \alpha_n b + \alpha_n b/\sinh \alpha_n b) + 4\alpha_n^{-2} q_n g \sinh \alpha_n b\}}. \tag{30}$$

EFFECTIVE WIDTHS

Effective width definition has traditionally been based on the distribution of longitudinal stress across the slab width. This definition takes effective width as the equivalent width of slab having a constant stress distribution across it and sustaining a force equal to the interacting axial force in each of the elements of the composite system. The magnitude of the constant stress is taken as the peak longitudinal stress in the slab at the slab-beam junction. Based on this definition, the effective width factor β is given by

$$\beta = \frac{\int_{-b}^{b} \sigma_{11}\, dy}{b \cdot \sigma_{11}|b}. \tag{31}$$

The current analysis has, however, exposed the inadequacy of this definition, since effective width values obtainable from it depends on the manner of distribution across the slab width of the longitudinal stress in the slab. The values of effective widths for partial interaction obtained from expression (31) decrease with increasing degree of interaction (see Table 2 for β). On the other hand, the middle-plane slab stress at the slab-beam junction increases with increasing degree of interaction, as would be expected from a physical conjecture. Notwithstanding this trend of growth of stress with increasing degree of interaction, the implication of decreasing effective width with increasing degree of interaction would be that less of the slab is participating in increasing the stiffness of the equivalent T-beam as interaction progresses. Such a phenomenon would be inconsistent with physical expectation and this short-coming points to the inherent weakness of this definition for effective width.

The alternative accepted definition of effective width based on deflexion has provided a trend that agrees with physical expectation and has been taken as the basis of calculating the effective width factors presented. Deflexion at the rib junction is determined by the "exact" analysis, giving;

$$w = \sum_{n=1}^{\infty} \cos \alpha_n x\{\alpha_n^{-4} q_n - \alpha_n^{-1} B_n(\cosh \alpha_n b + \alpha_n b/\sinh \alpha_n b)\}. \tag{32}$$

Assuming that each rib supports the point load on it together with the superimposed slab load between two ribs, then the deflexion of the equivalent section becomes

$$w = (E_s I_e)^{-1} \sum_{n=1}^{\infty} \cos \alpha_n x\left\{\alpha_n^{-4}\left[\frac{p}{a} + \frac{2(-1)^{n+1}}{\alpha_n a}(p_s + 2bq)\right]\right\} \tag{33}$$

where I_e is the equivalent second moment of area of the composite system. Equating the two deflexions, we have

$$E_s I_e = \frac{\sum_{n=1}^{\infty} \cos \alpha_n x \left\{ \alpha_n^{-4} \left[\frac{p}{a} + \frac{2(-1)^{n+1}}{\alpha_n a} (p_s + 2bq) \right] \right\}}{\sum_{n=1}^{\infty} \cos \alpha_n x \{ \alpha_n^{-4} q_n - \alpha_n^{-1} B_n (\cosh \alpha_n b + \alpha_n b / \sinh \alpha_n b) \}} \cdot \quad (34)$$

If it is assumed that the transformed section theory can still be applied to a partially interacting system, the effective width factor β_w, using the equivalent steel second moment of area and based on the transformed section theory, is given by

$$\beta_w^2 (2b^2 t^4) + \beta_w \{ A_s (3d^2 + 6dt + 4t^2) - 12(I_e - I_s) \} mbt - 6m^2 A_s (I_e - I_s) = 0. \quad (35)$$

Using transformed section theory, the values of effective widths obtained from deflexion consideration were used in calculating the maximum steel bottom flange stress for various side ratios and k_s. These values were then compared with the maximum stresses obtained from the analysis for the appropriate side ratio and k_s (see Table 1 for σ_{tr}/σ_{sb}).

Table 1. $\frac{\sigma_{tr}}{\sigma_{sb}}$

$\frac{100k_s}{E_s}$	$\frac{b}{a}$			
	0·4	0·6	0·8	1·0
0·0625	1·011	1·023	1·038	1·050
0·125	0·988	0·998	0·014	1·034
0·250	0·967	0·975	0·989	1·009
0·500	0·951	0·958	0·970	0·989
1·000	0·940	0·946	0·958	0·976
2·000	0·935	0·940	0·951	0·969
4·000	0·933	0·937	0·948	0·965

It is seen from this table that apart from values at low interaction, the values of the stresses obtained from the transformed section theory are generally lower than those obtained from the exact analysis for the same side ratio and interaction. Nevertheless, it is thought that this approximation by the transformed theory could still be applied since the values obtained when it is employed are generally over 90 per cent of the values from exact analysis.

Slip is expressed as a fraction of the maximum central deflexion for the particular interaction and side ratio. Figure 5 shows the familiar theoretical slip characteristics in composite beams, with the slip decreasing as k_s increases. The analysis shows that for full interaction to be attainable, k_s must be fairly large, i.e. of the order of 30 KN/mm^2. For practical purposes, however, a value of $k_s = 0{\cdot}04E_s$ should be adequate as a guide for full interaction.

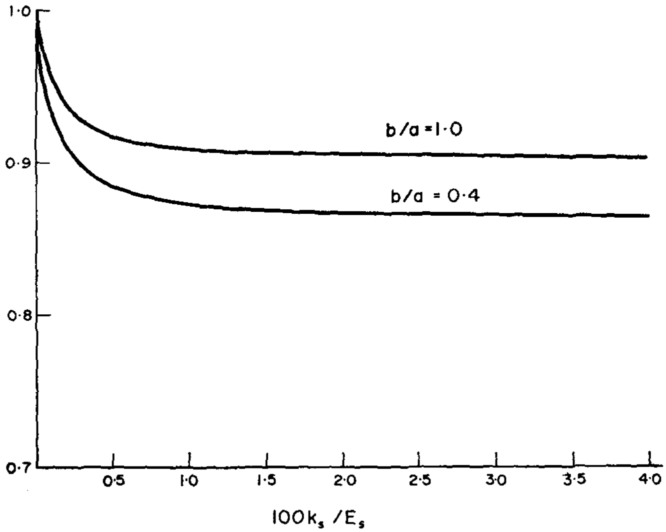

Fig. 4. Showing steel bottom flange stress reduction with increasing interaction.

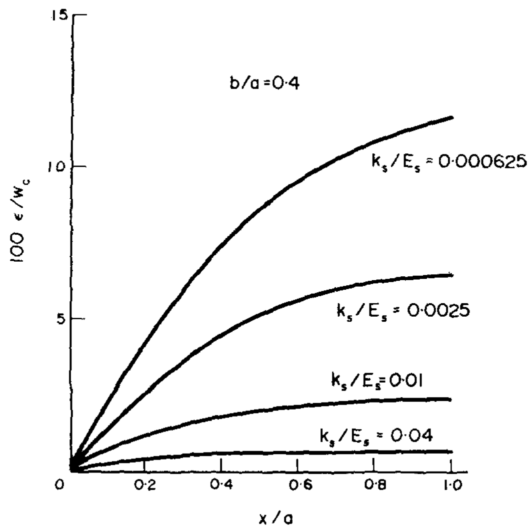

Fig. 5.

CONCLUDING REMARKS

The analysis has demonstrated the dependence on partial interaction of shear lag and has led to the conclusion that effective width concept ought really to be based on deflexion considerations rather than stress considerations.

Table 2 shows that effective width based on stress definition decreases from a higher value at low interaction to some limiting lower value at a high degree of interaction, although correspondingly the maximum slab middle-plane stress increases from zero at zero interaction to some limiting value at a high degree of interaction. These two obviously interrelated phenomena make one no wiser as to how these "stress" effective widths can

Table 2. For $b/a = 0{\cdot}4$

$\frac{100k_s}{E_s}$	β	$\frac{\sigma_{mp}}{\sigma_{mf}}$
0·0625	0·759	0·323
0·125	0·753	0·468
0·250	0·744	0·607
0·500	0·731	0·725
1·000	0·715	0·815
2·000	0·700	0·882
4·000	0·688	0·929

be judiciously used in design of *T*-beams at any interaction. On the other hand, the behaviour of the "deflexion" effective widths with increasing interaction lends itself to the concept of increased equivalent stiffness attributable to the increasing participation of the slab as interaction progresses. The transformed section theory will therefore validly give an approximation of that equivalent stiffness in terms of the effective width of slab.

The slight underestimate of stress obtained using transformed section theory in conjunction with deflexion effective width would seem not to need compensating in view of the manner of deciding design loads in everyday engineering practice and the factor of ignorance between actual working loads, and design loads.

Figure 4 shows that steel bottom flange stress is decreasing as interaction increases but reaches a limiting value quickly at a k_s value of $0{\cdot}015E_s$. This means that, from the point of view of steel bottom flange stress reduction, this value of k_s would be adequate for deciding a "pseudo" full-interaction situation. Much the same sort of reasoning can be applied to the deflexion factor curves (Figs. 2 and 3).

At high interaction, when for practical purposes the system could be assumed to be one of full interaction, effective width values to be used in computations could be taken as $\frac{1}{6}$ of span for aspect ratio of 0·4 and below $\frac{1}{5}$ of span for 0·6 and $\frac{1}{4}$ of span for 0·8–1·0.

The analysis shows, theoretically, that for full interaction to exist, k_s must attain an infinite value. This would mean an infinite number of connectors in a composite *T*-beam. The analysis has however demonstrated that the stresses and deflexions tend so quickly to limiting values that, for practical purposes, the k_s value need not exceed 2 per cent of E_s, although correspondingly slip may still exist appreciably and be of the order of 1·25 per cent of the central deflexion.

Acknowledgements—My thanks go to Dr. K. Aderogba, Lecturer in Engineering Analysis in the Department, who assisted with the mathematical simplification of the equations obtained, and also made a number of useful suggestions on the method of computation. My appreciation also goes to Mr. Johnson of the Shell BP Computer Centre in Lagos and Dr. J. O. Sonuga, Senior Lecturer in the Department, both of whom gave invaluable advice on the programming.

REFERENCES

1. S. Timoshenko and S. Woinowsky-Krieger, *Theory of Plates and Shells*. McGraw-Hill, New York (1959).
2. Chi-Teh Wang, *Applied Elasticity*. McGraw-Hill, New York (1953).
3. G. Petit Bois, *Table of Indefinite Integrals*. Dover Publications, New York (1961).
4. A. O. Adekola, Effective width of composite beams of steel and concrete. *Struct. Engr* **46** (9), 285–289 (1968).
5. A. O. Adekola, Partial interaction between the elastically connected elements of a composite beam. *Int. J. Solids Struct.* **4**, 1125–1135 (1968).

Абстракт — В работе формулируются определяющие уравнения, которые связывают частичное взаймодействие с запаздыванием сдвига. Уравнения решаются методом рядов, для определения прогиба и напряжений в плоскости стержня. Решения удовлетворяют всем известным граничным условиям. Результаты очевидно указывают влияние гибких соединителей сдвига, используемых в составных балках. Они, также, показывают, что с целью получения более рациональной базы для определения эффективной ширины надо обсуждать условия изгиба. Это значит, что эффективная ширина увеличивается с ростом степени взаимодействия, т. е. если увеличивается число гибких соединений сдвига. Доказывается, также, что существует крайная степень взаимодействия, выше которой прогиб заметно не оказывает значительного влияния.